

# Full-field mapping of ultrasonic field by light-source-synchronized projection

Gang Yao and Lihong V. Wang\*

*Biomedical Engineering Program, Texas A&M University  
233 Zachry Engineering Center, College Station, TX 77843-3120  
gyao@tamu.edu lwang@tamu.edu*

**Abstract:** A simple method for imaging ultrasonic fields in clear media is introduced. A modulated laser source is used to project the ultrasonic field onto a CCD camera. By use of the source-synchronized lock-in detection scheme, 2D images of the amplitude and phase distributions can be determined simultaneously. This technique is experimentally demonstrated with a 1-MHz and a 3.5-MHz ultrasonic transducer operated in continuous-wave mode. This method is very straightforward to implement and can be combined with the traditional tomographic reconstruction technique to obtain the 3D distribution of an ultrasonic field.

© 1999 Acoustical Society of America

**PACS numbers:** 43.58.-e, 43.20.Ye, 43.35.Sx

## Introduction

Because of the advantage of noninvasive measurements, various optical techniques, such as the Bragg diffraction,<sup>1</sup> Schlieren imaging,<sup>2</sup> Raman-Nath diffraction,<sup>3</sup> and TV holography,<sup>4</sup> have been used to map ultrasonic fields. Most of these methods except TV holography must use some scanning mechanisms to acquire an image. Using a speckle interferometer with a video camera in TV holography, one can measure the amplitude and phase information of an ultrasonic field simultaneously. TV holography has been successfully applied to the investigation of ultrasonic fields in clear media and water.<sup>5</sup>

In this letter, we demonstrate a simple method for mapping the projection of an ultrasonic field by using a source-synchronized parallel lock-in detection scheme.<sup>6</sup> The illuminating light is modulated at the frequency of the ultrasonic field. The pressure and phase distributions of a 1-MHz and a 3.5-MHz ultrasonic transducer operated in continuous-wave (cw) mode are obtained by this method. A comparison of the experimental and theoretical results is also provided.

## Method

The experimental setup is shown in Fig. 1. The ultrasonic transducer is immersed in a 10-cm x 15-cm x 15-cm glass tank containing clear water. A 5-cm thick rubber slab is placed at the bottom of the tank to prevent reflection of ultrasound from the bottom of the tank. The laser beam from a diode laser (693 nm, Melles Griot 56IMS667) illuminates the ultrasonic field after beam expansion. The transmitted light is projected onto the CCD camera (Dalsa CA-D1-0256T) through an imaging lens. Two function generators (Stanford Research Systems, DS345) are used to excite the ultrasonic transducer and modulate the diode laser, respectively. The two function generators share the same time base to ensure synchronization. The function generators and the CCD camera are controlled by a personal computer. The ultrasonic

---

\* Correspondence should be addressed to the second author at Tel: (409) 847-9040, Fax: (409) 845-4450, Email: lwang@tamu.edu

transducer is mounted on a translation stage which is movable vertically (along the X axis). By moving the transducer along the X axis, different segments of the ultrasonic field can be imaged.

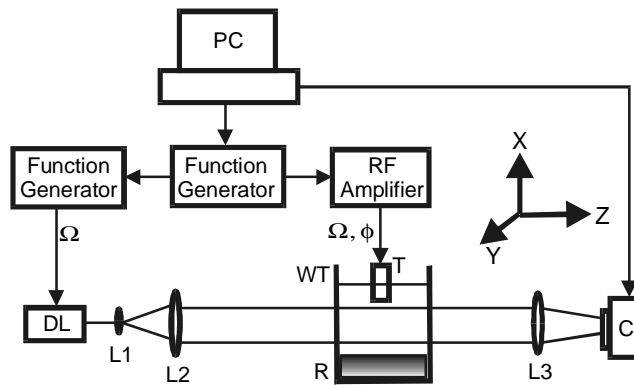


Fig. 1. Schematic sketch of the experimental setup for the measurement of ultrasonic fields in water. DL: diode laser; L1, L2, L3: imaging lens; WT: water tank; R: rubber slab; C: CCD camera; T: ultrasonic transducer.

A coordinate system is setup as shown in Fig. 1. The X axis is on the acoustic axis pointing to the ultrasonic transducer. The Y axis is perpendicular to both the acoustic and optical axes. The Z axis is along the optical axis pointing to the CCD camera.

The CCD camera is positioned before the focal plane of the imaging lens. In other words, we are working in the near-field region. In the Raman-Nath acousto-optic interaction regime, the near-field light intensity diffracted by an ultrasonic wave with frequency  $\Omega$  is:<sup>7,8</sup>

$$I(x, y, Z, t) = CI_i \left( 1 + 2 \sum_{n=1}^{+\infty} J_n [2v_{x,y} \sin(2n\pi Z)] \times \cos[n(\Omega t + \Phi_{x,y} + \varphi)] \right), \quad (1)$$

where  $I_i$  is the incident laser intensity,  $C$  is a constant,  $J_n$  is the  $n$ th order Bessel function of the first kind,  $v_{x,y}$  and  $\Phi_{x,y}$  are respectively the effective Raman-Nath parameter and the effective phase of the ultrasonic field along the projection path,<sup>5</sup>  $\varphi$  is the initial phase of the ultrasonic wave, and  $Z$  is a normalized parameter defined as:<sup>8</sup>

$$Z = (z - L) \times \lambda / (2n_0 \Lambda^2), \quad (2)$$

where  $L$  is the interaction length between the ultrasonic field and the light,  $\lambda$  and  $\Lambda$  are respectively the optical wavelength and the acoustic wavelength,  $n_0$  is the refractive index of the medium. The effective pressure  $P$  can be derived from the Raman-Nath parameter as:

$$P_{x,y} = \frac{v_{x,y} \lambda}{2\pi L (\partial n / \partial p)}, \quad (3)$$

where  $\partial n / \partial p$  is the piezo-optical coefficient of the medium.

The incident laser  $I_i$  intensity is also modulated at the frequency  $\Omega$ :  $I_i = I_0 + I_0 \cos(\Omega t)$ . The CCD camera acts as a low-pass filter because of its low running frequency relative to  $\Omega$ . Considering  $J_1(x) \cong x/2$  at small  $x$ , the signal detected by the CCD camera can be written as:

$$S_\varphi(x, y) = \langle I(x, y, Z, t) \rangle_t = CI_0 + C_1 I_0 v_{x,y} \cos(\Phi_{x,y} + \varphi), \quad (4)$$

where  $\langle I(x,y,Z,t) \rangle_t$  is the time average of the received light intensity in the exposure period of the CCD camera and  $C_1 = C \sin(2\pi Z)$ . In the experiment, the phase of the signal applied to the ultrasonic transducer is set sequentially to  $0^\circ, 90^\circ, 180^\circ, 270^\circ$  relative to the signal applied to the diode laser. The corresponding four frames of CCD images are acquired to calculate the amplitude and phase distributions of the ultrasonic field. The pressure-related Raman-Nath parameter  $v_{x,y}$  and the phase  $\Phi_{x,y}$  can be obtained as:

$$v_{x,y} = \frac{1}{2C_1 I_0} \sqrt{(S_{0^\circ} - S_{180^\circ})^2 + (S_{90^\circ} - S_{270^\circ})^2} \quad (5)$$

$$\Phi_{x,y} = -\tan^{-1} \frac{S_{90^\circ} - S_{270^\circ}}{S_{0^\circ} - S_{180^\circ}} \quad (6)$$

The Raman-Nath parameter can be converted to effective pressure by Eq. (3) if the piezooptical coefficient of the medium is known.

### Results and Discussion

In the experiment, a ruler placed on the acoustic axis is imaged by the CCD camera to calibrate the magnification of the system. Figure 2 shows the ultrasonic field of a 1-MHz transducer (Panametrics V314-1.0/0.75) operated in cw mode with a focal length of 2.54 cm. The gray-scale images are obtained by combining three images corresponding to different ultrasonic-field segments. In the amplitude image, white color refers to the higher intensity and black color the lower intensity. In the phase image, the phase is wrapped between  $[-\pi, +\pi]$ .

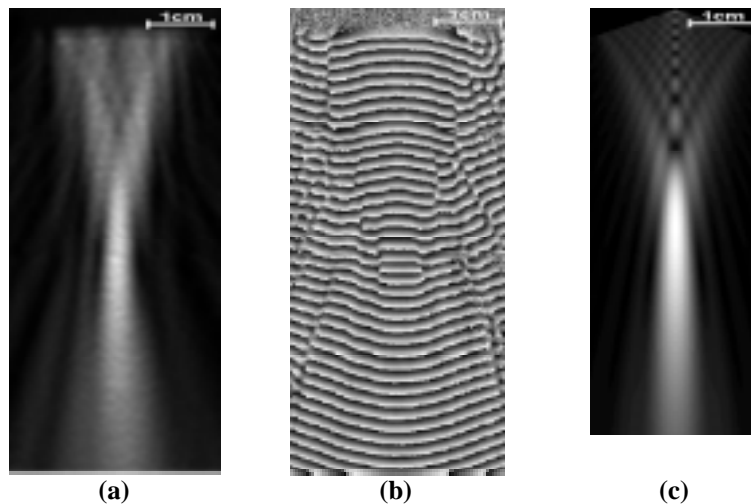


Fig. 2. 2D projection images of a 1-MHz ultrasonic field. (a) Experimental amplitude image; (b) experimental phase image; (c) theoretical amplitude distribution.

Figure 2(a) and 2(b) show the experimentally measured amplitude and phase distributions, respectively. Figure 2(c) shows the amplitude distribution calculated by the following equation:

$$p(\mathbf{r}, t) = C \int_s \frac{p(s) \exp[j(\Omega t - \phi)]}{d} ds \quad (7)$$

where  $p(\mathbf{r}, t)$  is the pressure as a function of the spatial position  $\mathbf{r}$  and time  $t$ ,  $C'$  is a constant,  $p(s)$  is the pressure distribution on the surface of the ultrasonic transducer,  $\Omega$  is the angular frequency of the ultrasonic wave,  $\phi$  is the phase delay between a point on the transducer surface and the observation point, and  $d$  is the distance between a point on the transducer surface and the observation point. The integration is over the surface of the transducer.

As shown in Fig. 2, the experimental result and the theoretically modeled result agree with each other very well in the far field. In the near field, the difference is caused by the projection nature of the experiment. In the projection measurement, the measured amplitude corresponds to an effective pressure along the optic projection line in the ultrasonic field. More accurate results can be obtained by reconstruction<sup>5</sup> as in the traditional tomographic measurements. Figure 3(a) shows the 1D amplitude profiles along the horizontal direction ( $Y$  axis in Fig. 1) at the focus point (2.54 cm) obtained experimentally and theoretically. The measured FWHM (full width at half maximum) of  $\sim 2.1$  mm is very close to the theoretical value of 2.2 mm. Figure 3(b) shows a plot of the phase along the acoustic axis of the transducer ( $X$  axis in Fig. 1). The measured period of the phase is  $\sim 1.43$  mm, which is close to the wavelength of 1-MHz ultrasonic wave in water (1.48 mm).

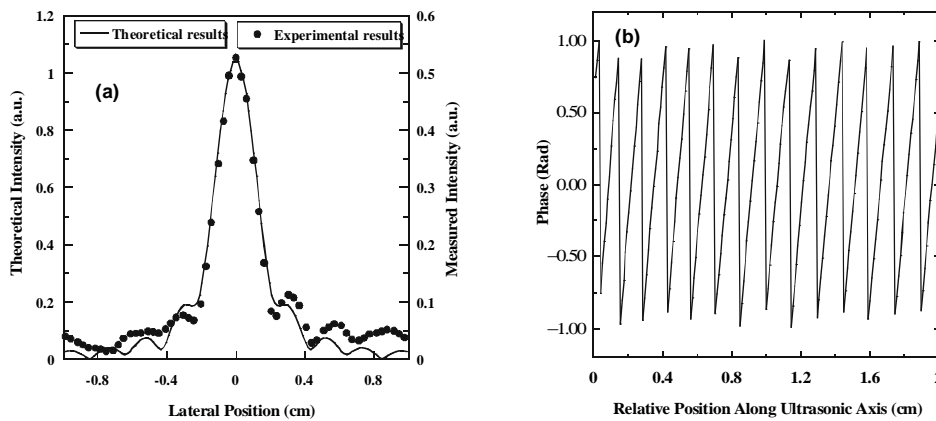


Fig. 3. 1D plots of the 1-MHz ultrasonic field. (a) Amplitude plot along the  $Y$  axis; (b) phase plot along the ultrasonic axis.

This method can also be applied to mapping ultrasonic fields of higher frequencies. The amplitude and phase distributions of a 3.5-MHz ultrasonic transducer are shown in Fig. 4 to demonstrate this point.

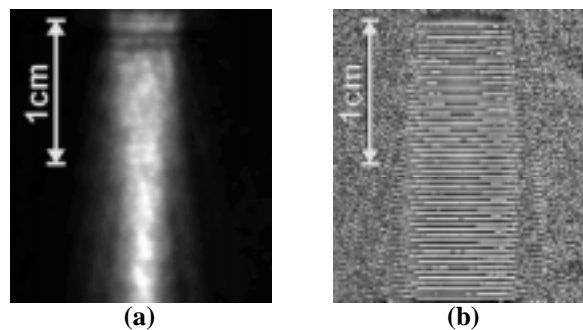


Fig. 4. 2D projection images of a 3.5-MHz ultrasonic field. (a) Amplitude image; (b) phase image.

## Conclusion

A simple method for investigating the ultrasonic field has been introduced in this letter. This method is based on a source-synchronized parallel lock-in detection scheme. The illumination light is modulated at the same frequency as the ultrasonic transducer and detected by a CCD camera after passing through the ultrasonic field. The amplitude and phase information can be measured simultaneously. This method can also be extended for tomographic measurements by rotating the transducer, which will furnish more accurate information. As with all other projection measurements, the application of this method is limited to weak acousto-optic interaction in which ray bending is negligible. Further theoretical studies as well as more accurate experimental calibration will be helpful for quantitative studies of ultrasonic fields by this method.

## Acknowledgments

This project was sponsored in part by the National Institutes of Health grants R29 CA68562, R01 CA71980 and R21 CA83760 and by the National Science Foundation grant BES-9734491.

## References and links:

- <sup>1</sup> A. Korpel, L. W. Kessler, and M. Ahmed, "Bragg diffraction sampling of a sound field," *J. Acoust. Soc. Am.* **51**, 1582-1592 (1972).
- <sup>2</sup> B. R. Barnes and C. J. Burton, "Visual methods for studying ultrasonic phenomena," *J. Appl. Phys.* **20**, 286-294 (1949).
- <sup>3</sup> R. Reibold and W. Molkenstruck, "Light diffraction tomography applied to the investigation of ultrasonic fields. I: continuous waves," *Acoustica* **56**, 180-192 (1984).
- <sup>4</sup> S. Ellingsrud and G. O. Rosvold, "Analysis of a data-based TV-holography system used to measure small vibration amplitudes," *J. Opt. Soc. Am. A* **9**, 237-251 (1992).
- <sup>5</sup> R. Rustad, "Acoustic field of a medical ultrasound probe operated in continuous-wave mode investigated by TV holography," *Appl. Opt.* **37**, 7368-7377 (1998).
- <sup>6</sup> P. Gleyzes, F. Guernet and A. C. Boccara, "Picometric profilometry. II. Multidetector approach and multiplexed lock-in detection," *J. Opt.* **26**, 251-265 (1995).
- <sup>7</sup> B. D. Cook, "Measurement from the optical nearfield of an ultrasonically produced phase grating," *J. Acoust. Soc. Am.*, **60**, 95-99 (1976).
- <sup>8</sup> E. Blomme and O. Leroy, "Plane-wave analysis of the near field of light diffracted by ultrasound," *J. Acoust. Soc. Am.*, **91**, 1474-1483 (1992).